CEP signal to background separation with the CMS Precision Proton Spectrometer at the HL-LHC

Johanna Lömker

August 20, 2021

Abstract

This report contains the first feasibility study of the signal to background separation for Central exclusive production with the CMS Proton Precision Spectrometer (PPS) at the HL-LHC. In the framework of the CERN Summer Student program 2021 the study has been performed with simulated proton-proton collisions at $\sqrt{s} = 14$ TeV. The goal was to define a selection procedure to discriminate between protons coming from pile-up collisions combined with the signature of the Drell-Yan background process $pp \to Z \to \mu^+\mu^-$ and pairs of protons coming from the signal $pp \to \mu^-\mu^+p'p'$. The project includes two possible scenarios of PPS timing resolution of 50 ns and 20 ns and reports the relative sensitivity for CEP signals at the HL-LHC.

Contents

1 Introduction **2**

2 Experimental specialty **3**

3 Theoretical relations **4**
3.1 Kinematic correlations . . . 4
3.2 Timing correlation . . . 4
3.3 Figure of merit . . . 5

4 Event selection **5**
4.1 Signal and background samples . . . 5
4.2 Object selection . . . 6
4.2.1 Smearing kinematic variables . . . 7
4.2.2 Smearing time variables . . . 7
4.2.3 MIP timing detector (MTD) resolution . . . 7
4.3 Signal selection . . . 8
4.3.1 Kinematic selection cut . . . 8
4.3.2 Timing selection cut . . . 9

5 Results **10**
5.1 Kinematic selection . . . 10
5.2 Timing selection . . . 11
5.3 Combine kinematic and timing selection . . . 13
5.4 Full selection . . . 14
5.5 Summary and conclusion . . . 15

6 Acknowledgements **16**

1 Introduction

The central exclusive production (CEP) of pair of leptons using the CMS Proton Precision Spectrometer (PPS) has been studied previously [1] with the run 2 data, with an integrated luminosity of 9.6 fb^{-1}. The future HL-LHC aims to deliver proton proton collisions at 14 TeV with an integrated luminosity of 3000 fb^{-1} for the upgraded CMS experiment. With the CMS upgrade, which includes an additional timing detector for the measurement of minimum ionizing particles (MIPs) that travel from the central collision point through the barrel (The MIP timing detector - MTD), a new possibility for a more accurate signal to background separation emerges. The CEP of muon pairs $pp \to \mu^-\mu^+pp$ as depicted on the left in figure 1 is a rare process (typical production cross-section of $\approx 100fb$) that is in principle easy to tag due to the special signature. The interacting protons scatter and transfer a small fraction of energy to produce two muons. The protons will lose a fraction of energy, as indicated by the p, but they will stay intact and travel slightly deflected to the beam. This deflection from the main beam allows the detection with the (forward and backward) PPS detectors on both sides of the CMS experiment.

The largest background comes from Drell-Yan ($Z \to \mu^+\mu^-$) events in the central detector, combined

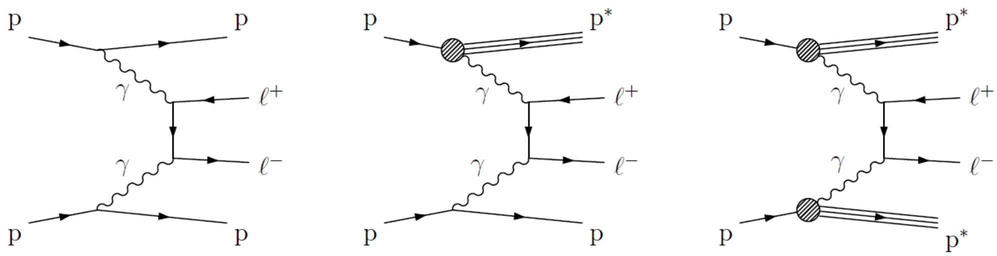

Figure 1: Simulated process $pp \to \mu^-\mu^+pp$: Production of lepton pairs by $\gamma\gamma$ fusion. The exclusive (left), single proton dissociation or semi-exclusive (middle) and double proton dissociation (right) topologies are shown. The left and middle processes result in at least one intact final-state proton, and are considered signal in this analysis. The rightmost diagram is considered to be a pile-up "like" event [1].

with energetically unrelated pileup protons. During one bunch crossing multiple pile up collisions occur. In $\approx$ 10%of the proton-proton collisions, there will be double diffractive and in 12% single diffractive processes where protons can stay intact but lose some fraction of energy. Additional protons can originate from the beam itself or other secondary processes, for example decays from diffractive processes. With the HL-LHC upgrade a pile up multiplicity up to 200 is assumed. All these pile up events give rise to additional protons which can be combined with the Drell-Yan ($Z \to \mu^+\mu^-$) background signature to mimic the CEP signal. But unlike the CEP signal, the background muons and pileup protons are not energetically correlated. The vertex position if z of di-muon production is reconstructed from the muon tracks in the CMS tracker and from the proton times of arrival in the PPS. The Phase 2 CMS upgrade project will involve MIP timing detector (MTD), which will provide additional timing information that to be used to suppress background events with the timing information from the PPS. The math behind this is shown in Chapter 8.1.4 of [2], but it has never before been studied in simulations for any specific physics process at HL-LHC. With the improved timing resolution of the PPS and the new timing detector narrower signal correlations and thus a better background rejection is expected.

The goal of the project was to define a selection procedure to discriminate between protons coming from pile up and background events and pairs of protons coming from the signal $pp \to \mu^-\mu^+pp$ and to estimate the signal to background separation at the HL-LHC.

First this report briefly introduces the experimental specialty in section 2. Then the theoretical relations and correlations, which are crucial for the signal selection, are defined in section 3 before the section 4 summarises the signal and background simulations, pre-selections and assumptions of the project. After that the most relevant correlations and the resulting selection cuts are shown for the two PPS timing resolutions (20ps and 50ps) in the results section 5. A short summary of the results for the station 1-3 and 1-4 scenario and a conclusion of the project are given in the end.

2 Experimental specialty

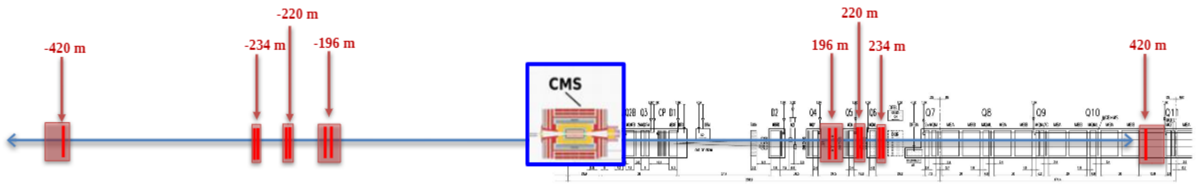

Figure 2: CT-PPS setup from [2]

(a) MTD design from [3]

(b) CMS slice from [4]

Figure 3: The CMS at HL-LHC

The general setup with the CMS detector (at IP5) between the PPS Roman pots (in sector 45 and 56) is shown in figure 2. For the CEP process the muon tracks are reconstructed from the silicon tracker and muon chambers as depicted in figure 3b. A time measure will be provided by the minimum ionizing particle timing detector (MTD figure 3a) with an targeted time resolution of 30-40ps. After the CMS central detector readout a 4-dimensional (spatial and timing) primary vertex is reconstructed and can be correlated to the vertex position and timing that is also reconstructed from the PPS data. The PPS detectors (Roman pots figure2) are currently located about 200-220m away from CMS on both sides of the LHC tunnel. After Run 3 they will be removed and reinstalled at a different location. Currently the tracking stations consist of 3D Si pixels which are used to measure the position of the protons in x and y coordinates relative to the beam. The deflection can be related to the fractional momentum ξ. When both protons in a $pp \to pXp$ process are detected, the mass and rapidity and position of the central system X can be calculated from the proton momentum lossξs. For protons that travel at very small angles relative to the beam, the vertex position can not be reconstructed from the tracking information alone. Therefore a timing station with diamonds is employed to measure the time-of-flight (ToF) of the two protons. The difference of the ToF can be used to find the z vertex position: two protons come from a collision exactly in the center of CMS (z=0), then travelling at the speed of light they will both arrive at PPS at the same time. If they come from a vertex with $z > 0$ the right proton will arrive before the left one, and vice versa. This report considers mostly the HL-LHC scenario including an additional PPS tracking station at $\approx$ 400m [2], which benefits the analysis. Only 3 stations will be in run 4 while the 4th station will be added at LS4. The PPS time resolution is expected to be 50ps for run 3 and the target for the HL-LHC is around 20ps. Even though the focus lies on the additional station 4 scenario, the station 1-3 case will be taken into consideration for the final result as well.

3 Theoretical relations

Due to energy conservation the measurable constituents of the CEP signal will be highly correlated. The correlations used for the run 2 analysis are the kinematic variables M (invariant mass) and Y (rapidity). With the HL-LHC and the CMS upgrade the vertex position and time correlation from the CMS and PPS measurements can be used in addition. The correlations allow to define signal selection cuts which will be introduced in section 4.

3.1 Kinematic correlations

All energy available for the central system comes from the protons momentum loss $\xi = \frac{p'-p}{p} = \Delta p/p$. The invariant mass and rapidity can be calculated from the decay products (di-muon system) of the central system and from the $\xi_{1,2}$ variables of the protons:

$$M_X = \sqrt{\xi_1 \cdot \xi_2}\sqrt{s} \tag{1}$$

$$|Y_X| = \frac{1}{2}\log(\xi_1/\xi_2). \tag{2}$$

The difference between the mass M_X and the rapidity $|Y_X|$ calculated from protons and from the di-muon system are used to define the kinematic selection in section 4.3.1. To analyse a realistic scenario the generated ξ values are smeared in section 4.2.1, following the expression of interest (EoI) [2].

3.2 Timing correlation

To calculate the protons true time of arrival at the PPS it is assumed that the protons both travel at the speed of light. The time when the protons should arrive at the PPS Roman Pots after propagating through the beam line in opposite directions can be calculated from generated values as depicted in figure 4. With the, from the CMS reconstructed, time and vertex position of the muons and the "reconstructed" (after smearing in section 4.2.2) time of the two protons there are two options to look for a correlation. Following the the expressions in the EoI [2]:

Vertex position in space:

$$rec\_vertex, z_{pp} = (t(p_1) - t(p_2))\frac{c}{2} \tag{3}$$

Vertex position in time:

$$(t(p_1) + t(p_2))\frac{c}{2} = z_{PPS} + (t_{MTD}(\mu_1) + t_{MTD}(\mu_2))\frac{c}{2} \tag{4}$$

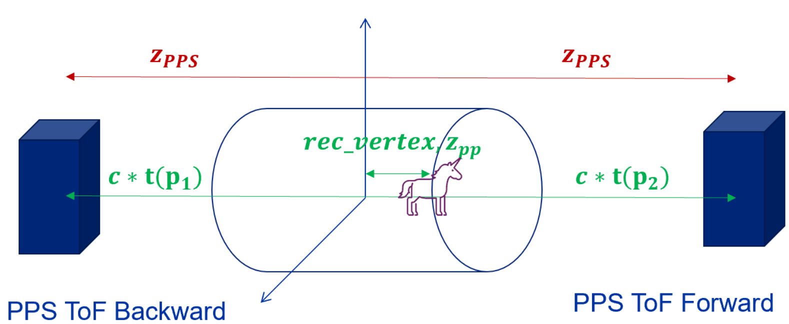

Figure 4: Vertex reconstruction of the "unicorn" CEP event from the proton times

3.3 Figure of merit

To compare the results of the signal to background separation with the previous analysis [1] the significance of selecting correctly identified signal events over the background estimate is calculated:

$$S = \frac{N_{Total}}{N_{Signal}} \tag{5}$$

with "Total" as the number all of selected events and "Signal" as the number of selected signal events. For a more reliable result the significance for each toy experiment is calculated and the average and standard deviation are derived from a Gaussian fit.

4 Event selection

Before selection cuts can be defined, the MC simulated signal and background data has to be pre-selected to construct toy experiments. The construction of the toy experiments includes realizable PPS acceptances for the proton measurement and the calculation of variables that are used for the signal selection.

4.1 Signal and background samples

The following processes were simulated to model signal and background events:

Signal

- 14 TeV $\gamma\gamma \rightarrow \mu^+\mu^-$
- $p_T(\mu) > 25$ GeV
- 600 events total
- Pile up multiplicity: 200
- Generator-level cross section (FPMC) = 0.2735 pb

Background

- 14 TeV Drell-Yan $Z \rightarrow \mu^+\mu^-$
- $p_T(\mu) > 2.5$ GeV and $|Y(\mu)| < 4.0$
- 15296 events total
- Pile up multiplicity: 200
- Generator-level cross section = 2.213 nb (Pythia8 CP5 - TBC)

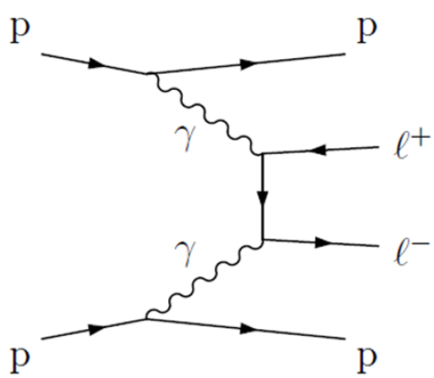

(a) Signal event, [1]

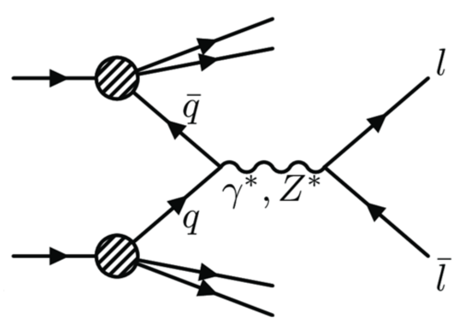

(b) Drell-Yan background, [5]

4.2 Object selection

Before any thresholds can be derived from the signal input, the signal and background sample are pre-selected in terms of the event kinematics, existing MTD data, the two PPS ξ acceptances from the station 1-3 and station 1-4 scenario and the two PPS timing resolutions (20ps and 50ps):

1. Selecting the two muons with highest transverse momentum $p_T > 25GeV$ and a valid time measurement $> -80ns$
2. Applying di-muon cuts according to the minimal ξ PPS acceptance for the planned installation (vertical crossing angle) from table 4 of the EoI [2]:
   - **Station 1-3**: $\xi_{\pm\mu\mu} > 0.01$ for an efficiency of $\approx 1.6\%$ (10/600) events
   - **Station 1-4**: $\xi_{\pm\mu\mu} > 0.0032$ for an efficiency of $\approx 17\%$ (106/600) events

   After the first two pre-selection steps the signal data is strongly reduced for the station 1-3 scenario. The little acceptance range does not allow a reliable study for this scenario, as demonstrated by the figure 6.

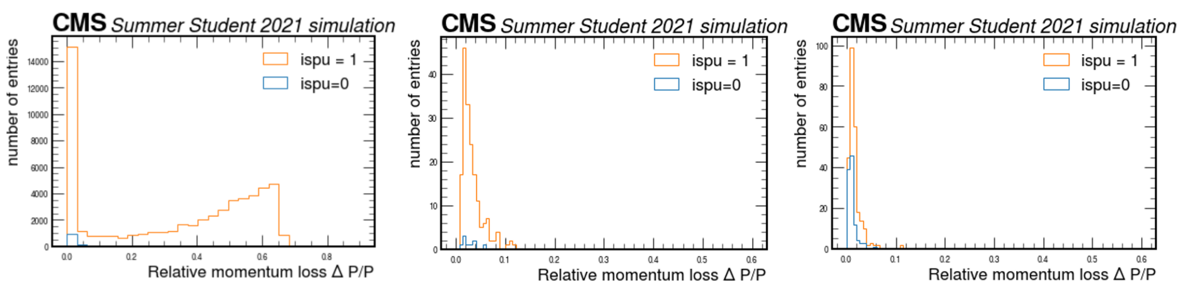

Figure 6: Relative momentum loss of signal (ispu = 0) and pile up (ispu = 1) protons. (Left) before any pre-selection cuts, after the first three steps of the pre-selection for the station 1-3 scenario (center) and for the station 1-4 scenario (right).

3. Smearing (equation 6) of proton pz by updating the ξ and p_z values for 2% resolution
4. Selecting two protons (equation 7) within the ξ_{min}, ξ_{max} PPS acceptance from table 4 of the EoI [2]:
   - **Station 1-3**: $\xi_{min} > 0.01$ & $\xi_{max} < 0.287$; efficiency $\approx 1.6\%$ (10/600) signal events
   - **Station 1-4**: $\xi_{min} > 0.0032$ & $\xi_{max} < 0.287$; efficiency $\approx 17\%$ (104/600) signal events
5. Storing the muon and proton data
6. Calculating the perfect proton times for the signal (equation 8) and background (equation 9)
7. Smearing (equation 10) the proton times according to the PPS resolutions (20ps and 50ps).

The pre-selected data can be used to approximate the MC simulated MTD timing resolution as described in section 4.2.3.

4.2.1 Smearing kinematic variables

The input data from section 4.1 contains the muon data simulated for the resolutions that are expected for the HL-LHC run. The proton data on the other hand is not fully simulated and has to be smeared according to the targeted PPS acceptances defined in the EoI [2].

$$xi\_smear = Gauss(0, (proton\_xi)) * xi\_res) \tag{6}$$

Draw random samples from a normal (Gaussian) distribution around 0 with standard deviation of resolution ($xi\_res = 0.02 = 2\%$ for now) times relative proton momentum loss.

$$proton\_xi = proton\_xi + xi\_smear$$
$$proton\_pz = proton\_pz + 7000 * xi\_smear$$

$$sel\_proton\_idx = (proton\_pz > pz\_min)\&(proton\_pz < pz\_max) \tag{7}$$

With $pz\_min = 4990$ and $pz\_max = (1 - \xi_{min}) * 7000$

4.2.2 Smearing time variables

For the analysis the single proton times can be calculated from the perfectly generated proton vertex positions. To assure a realistic scenario the obtained times are smeared according to the two targeted PPS timing acceptances and further used in section 4.3.2 to calculate the, in terms of the PPS resolution, realistic vertex position with the equation 3.

$$t_{sig,proton} = t_0 + (z_{PPS} - z_{proton})/c \tag{8}$$

With $zpps = 23400cm$ and $c = 29.979cm/ns$.

$$t_{bg,proton} = Gauss(0, 0.019) + (z_{PPS} - z_{proton})/c \tag{9}$$

It is stated in section 8.1.4 [2] that, to first order, the proton bunch profile is gaussian with beam width of 8.1 cm. The corresponding resolution is $\frac{0.271}{\sqrt{s}} = 0.019$ ns/TeV.

$$proton\_t = proton\_t + Gauss(0, resolution) \tag{10}$$

For the the two PPS time resolution of the "ideal" (20ps) and "modest" HL-LHC scenario (50ps).

4.2.3 MIP timing detector (MTD) resolution

To address the high pileup environment at the HL-LHC, the CMS collaboration is planning to add a timing layer (figure 3a) that will measure minimum ionizing particles (MIPs) with a time resolution of 30–40 ps, referred as the MIP Timing Detector (MTD).

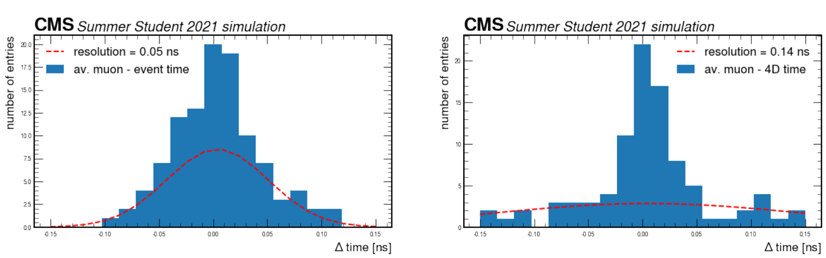

Figure 7: Simulated MTD timing resolution with (left) 'average muon time - event time' and (right) 'average muon time - 4D primary vertex time'

With the averaged muon time ($t_{di-\mu} = 0.5 \cdot (t_{\mu 1} + t_{\mu 2})$) and the primary vertex time, we can fit a Gaussian to approximate the realistic timing detector resolution that is MC simulated for this project.

The resolution is measured in percent and defined by the standard variation of the difference between reconstructed and true values:

$$\sigma^2 = \frac{1}{N-1} \sum (t_{rec} - t_{true})^2 \tag{11}$$

Figure 7 shows the plot of the MTD timing resolution as obtained from the MC simulation after the pre-selection. The Gaussian fits visually underestimate the data, but the results in terms of the resolutions assure that the pre-selected signal data does not overestimate the realizable or targeted MTD resolution for the HL-LHC.

4.3 Signal selection

Due to energy conservation the signal data from the muons and the protons will be highly correlated. For the signal to background separation the kinematic and timing correlations from the signal sample are used to derive selection cuts. The following sections will illustrate some of the correlations and how the selection cuts are derived.

4.3.1 Kinematic selection cut

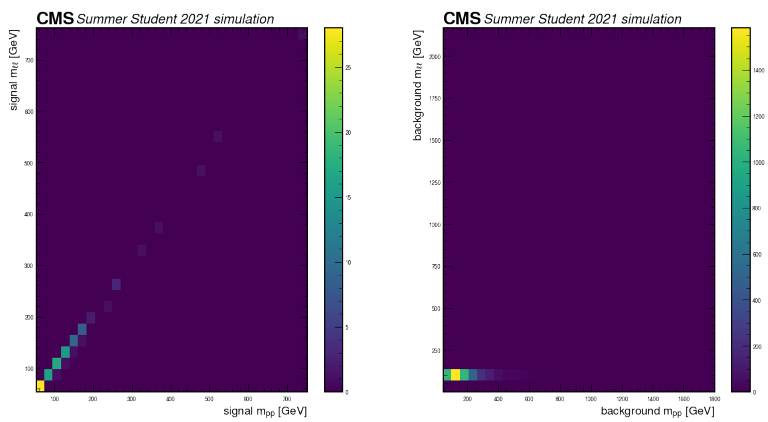

Figure 8: Correlation between the invariant mass calculated from the protons and the di-muon system for the signal and background

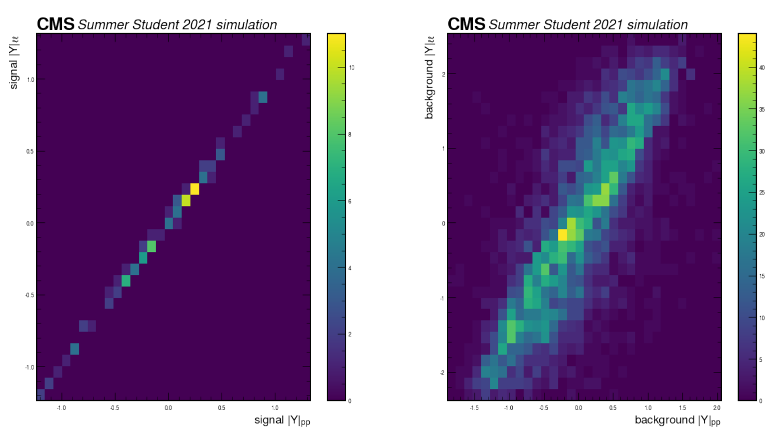

Figure 9: Correlation between the rapidity calculated from the protons and the di-muon system for the signal and background

The invariant mass and rapidity of the central system are calculated from the di-proton system as in section 3.1. Figure 8 and 9 show the nearly perfect correlation between the signal data coming from the CMS and PPS input. The background data is as expected uncorrelated. The narrow correlation between the CMS (muon) and PPS (proton) reconstructed data allow to set a tight cut for the kinematic signal selection.

Kinematic selection criteria from signal input

$$M_{fit} = \frac{m_{pp}}{m_{\ell\ell}} - 1 \tag{12}$$

$$|m_{pp} - m_{\ell\ell}| < |2 \cdot \sigma_m \cdot m_{\ell\ell}| \tag{13}$$

$$Y_{fit} = \frac{Y_{pp}}{Y_{\ell\ell}} - 1 \tag{14}$$

$$|Y_{pp} - Y_{\ell\ell}| < |2 \cdot \sigma_{|Y|} \cdot Y_{\ell\ell}| \tag{15}$$

The normalized differences in mass (equation 12) and rapidity (equation 14) from the di-muon (CMS) and di-proton (PPS) variables are fitted to a Gaussian as demonstrated in figure 10. The obtained resolution σ_i serves according to equation 13 and 15 as selection criteria to separate the signal events from the large background. The comparison of figure 10 with the figures 9 and 8 illustrates that a narrower correlation leads to a tighter selection criteria.

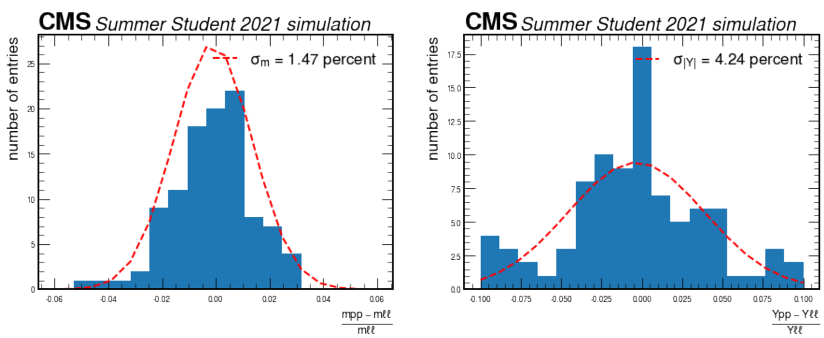

Figure 10: Input data from equation 14 and 12

4.3.2 Timing selection cut

Similar as in the previous step the correlation from section 3.2 of the two time measurements at the CMS and PPS can be used to define two more selection cuts. With equation 3 and 4 the vertex position and time from the central system can be reconstructed. The proton times are calculated from the "perfect" generated proton data and smeared according to the PPS resolution (20ps and 50ps) as in section 4.2.2. Then the realistic, in terms of the PPS resolution, proton vertex position is obtained from equation 3. The difference of the vertex position (equation 16) in z, calculated from the protons (PPS) and the primary vertex (CMS), give the third and previously approved selection cut (equation 17). New is the selection cut (equation 19) based on the vertex time difference (equation 18) from the averaged proton (PPS) and muon (MTD in CMS) data. The differences are both fitted to a Gaussian to obtain the σ_i for the selection cut but now in units of [cm] and [ns].

Timing selection criteria from signal input

$$Vtx(z)_{fit} = z^{pp}_{vtx} - z^{4D}_{vtx} \tag{16}$$

$$|z^{pp}_{vtx} - z^{4D}_{vtx}| < |2 \cdot \sigma_{vtx}| \tag{17}$$

$$T_{fit} = t(pp) - t(\mu^+\mu^-) \tag{18}$$

$$|t(pp) - t(\mu^+\mu^-)| < |2 \cdot \sigma_t| \tag{19}$$

5 Results

Each selection criteria has some impact on the number of selected signal and background events. To demonstrate the advantages of each selection the result of each criteria is presented separately and combined with the others, in the order of applied selection, for the 50ps and 20ps PPS timing resolutions. The full selections have been performed for the station 1-3 and 1-4 scenario, but the low efficiency from the section 4.2 (6) supports the detailed analysis with the additional station 4 scenario.

5.1 Kinematic selection

Figure 11 and 12 demonstrate that the narrow mass correlation (figure 8) does lead to a tighter selection cut (figure 10) and thus to a better signal to background separation. The combination of the two kinematic cuts allows an even better signal to background separation. The product of the separated acceptance rates (figure 11 and 12) are in rough agreement with the combined cut (figure 13). The different acceptances originate probably from double exclusion.

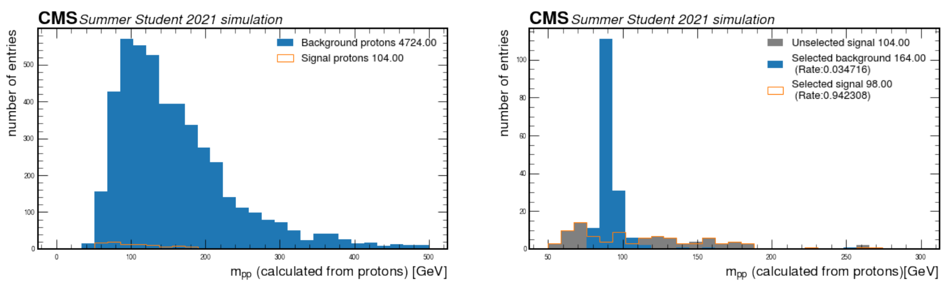

Figure 11: (Left) signal and background distributions after the pre-selection. (Right) the result of the invariant mass cut equation 13 of the central system (equation 1).

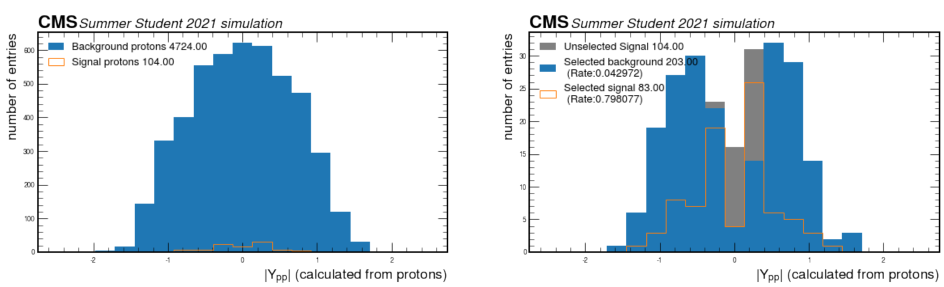

Figure 12: (Left) signal and background distributions after the pre-selection. (Right) the result of the rapidity cut equation 15 of the central system (equation 15).

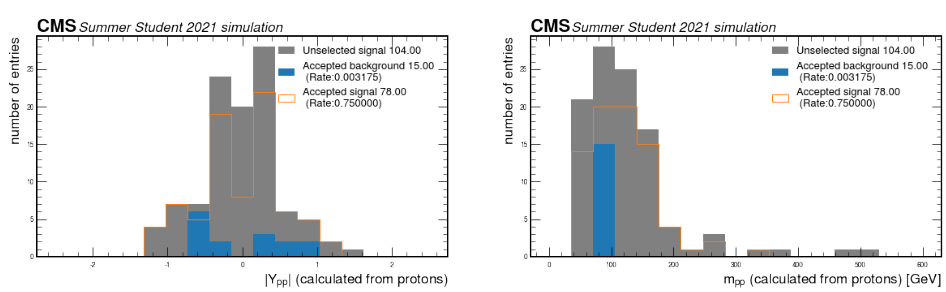

Figure 13: The accepted signal and background after 1. applying the rapidity and 2. the mass cut.

5.2 Timing selection

The single and combined results from the timing selection for the modest PPS time resolution of 50ps select more background events compared to the kinematic selection. To obtain a better background exclusion and signal acceptance the timing selection has to be performed with a better PPS timing resolution as presented in the following.

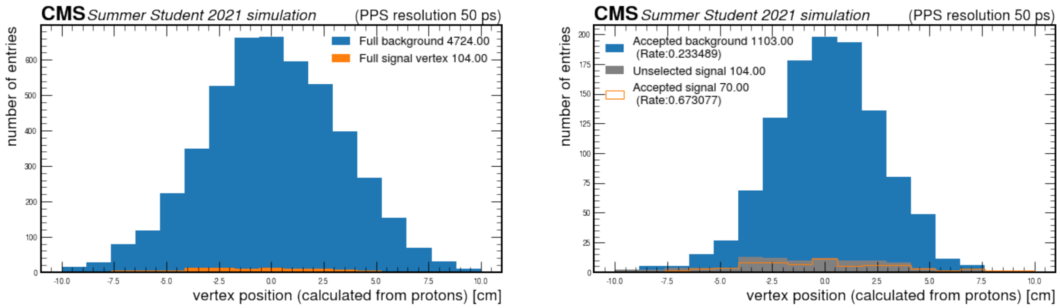

Figure 14: (Left) signal and background distributions after the pre-selection. (Right) the result of the vertex position cut (equation 17) for the PPS time resolution 50ps.

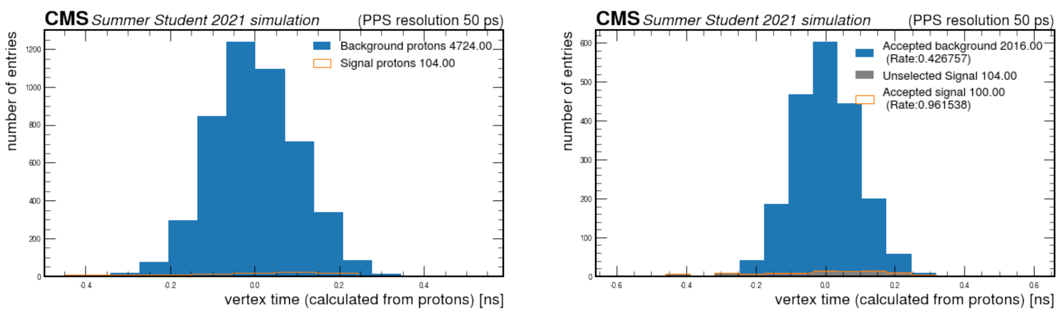

Figure 15: (Left) signal and background distributions after the pre-selection. (Right) the result of the vertex time cut (equation 19) for the PPS time resolution 50ps.

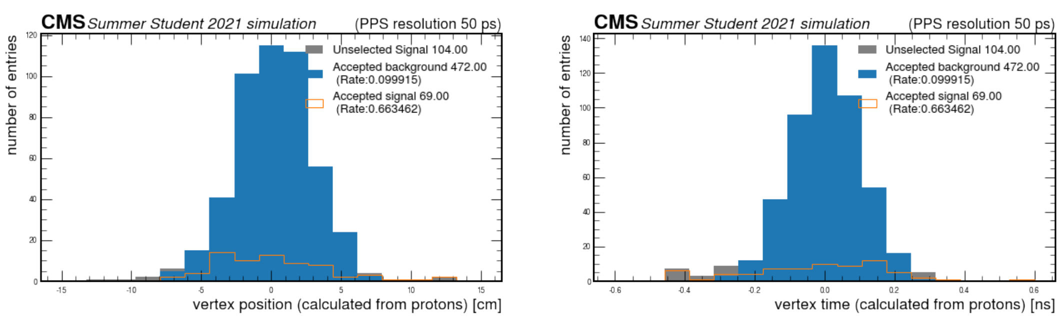

Figure 16: The accepted signal and background after 1. applying the vertex position (equation 17) and 2. the vertex time (equation 19) cut for the PPS time resolution 50ps.

The single and combined results from the timing selection for the ideal PPS time resolution of 20ps selects less background events compared to the modest PPS time resolution, but the improved resolution is not sufficient to correctly separate the signal events from the background. Therefore the combinations of the timing and kinematic cuts are required.

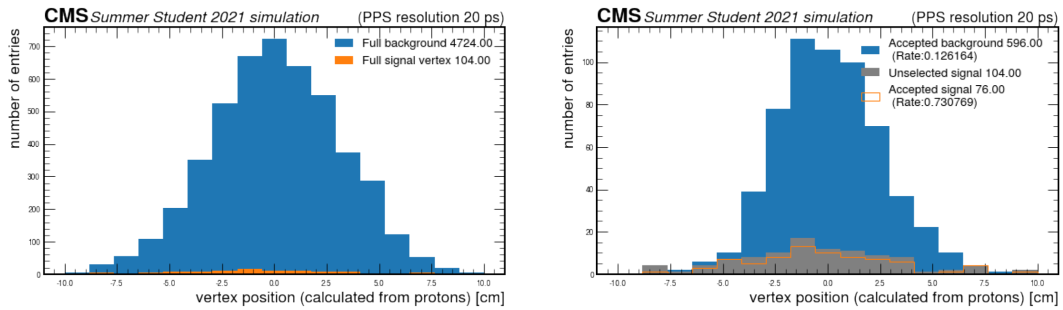

Figure 17: (Left) signal and background distributions after the pre-selection. (Right) the result of the vertex position cut (equation 17) for the PPS time resolution 20ps.

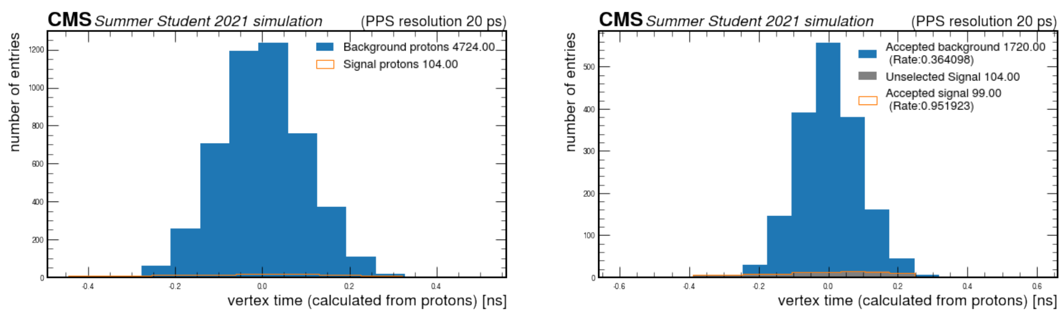

Figure 18: (Left) signal and background distributions after the pre-selection. (Right) the result of the vertex timing cut (equation 19) for the PPS time resolution 20ps.

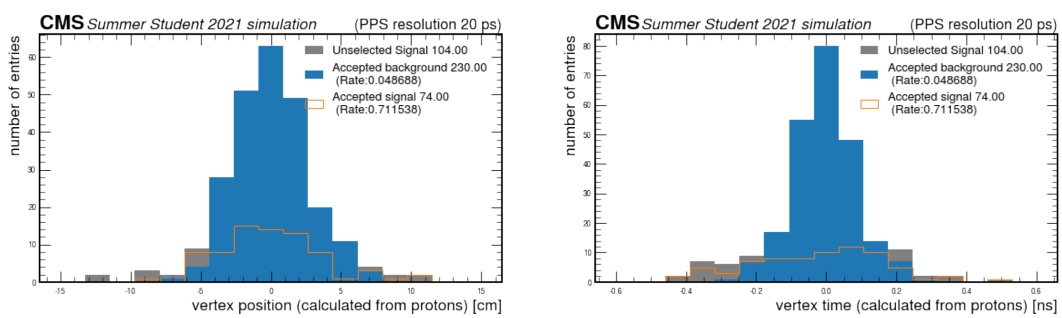

Figure 19: The accepted signal and background after 1. applying the vertex position (equation 17) and 2. the vertex time (equation 19) cut for the PPS time resolution 20ps

5.3 Combine kinematic and timing selection

It is interesting to note that the already previously (run 2 [1]) used cuts, based on the vertex position, can already lead to a full background exclusion for the ideal PPS time resolution (figure 22) but not for the modest time resolution. In each of case the combination of three cuts improves the signal to background separation.

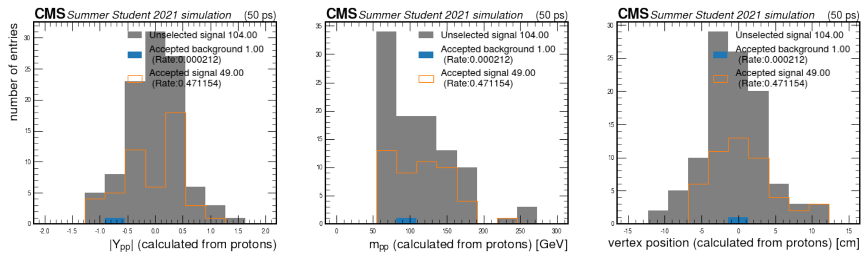

Figure 20: Combining the cuts from the equations 15, 13, 17 for the PPS time resolution 50ps.

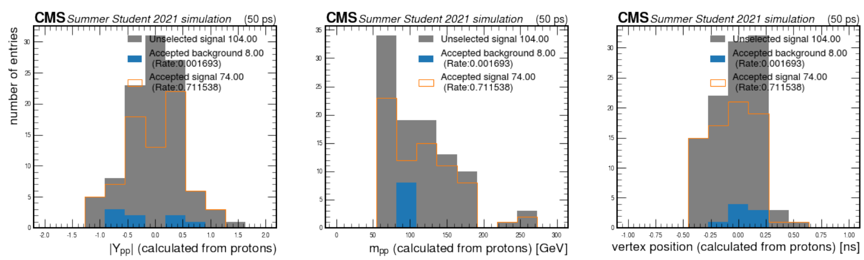

Figure 21: Combining the cuts from the equations 15, 13, 19 for the PPS time resolution 50ps.

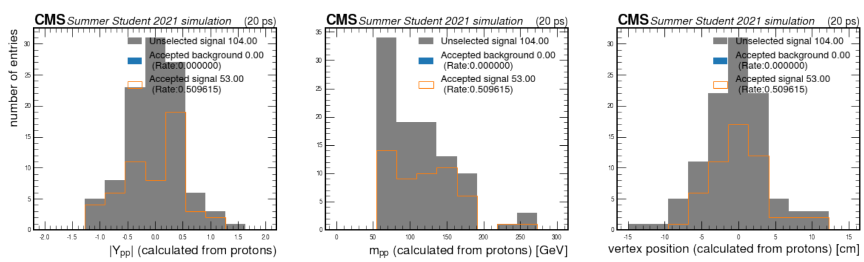

Figure 22: Combining the cuts from the equations 15, 13, 17 for the PPS time resolution 20ps.

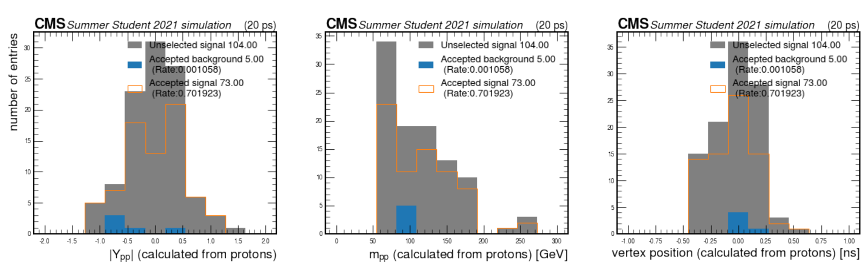

Figure 23: Combining the cuts from the equations 15, 13, 19 for the PPS time resolution 20ps.

5.4 Full selection

For both PPS timing resolutions the signal can be perfectly separated from the background with the full selection. The better resolution from figure 25 results in a higher acceptance for the signal data and thus better statistics for further analysis of the CEP. But since the pre-selection includes a lot of smearing, a full background exclusion cannot always be achieved.

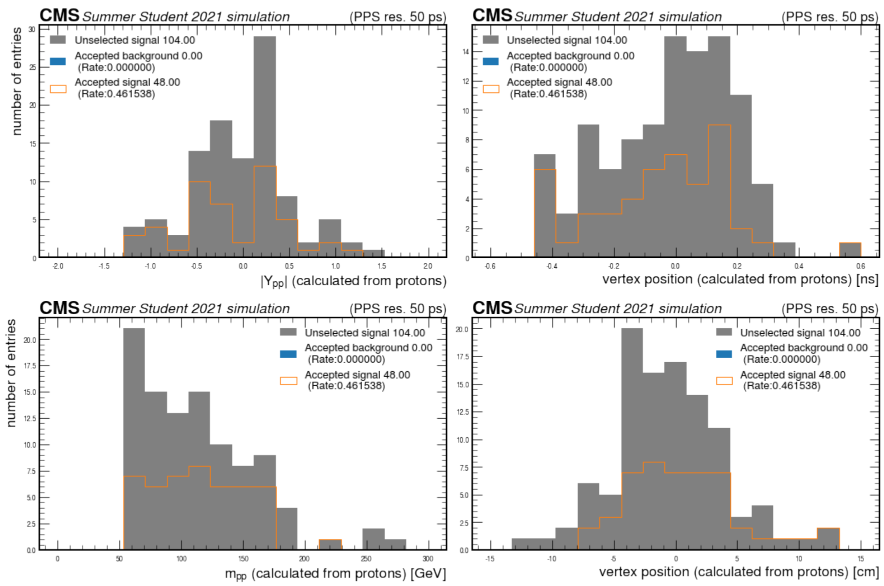

Figure 24: Combining all selection cuts from equations 15, 13, 19 and 17 for the PPS time resolution 50ps.

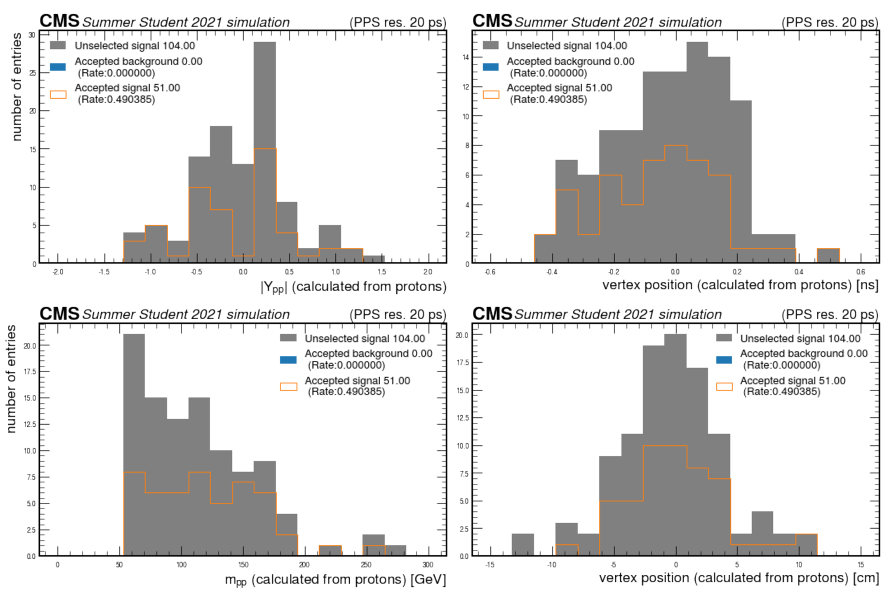

Figure 25: Combining the all selection cuts from the equations 15, 13, 19 and 17 for the PPS time resolution 20ps.

5.5 Summary and conclusion

The combination of the vertex position and the kinematics cuts can already lead to a full background exclusion for the ideal PPS resolution within the additional station 4 scenario. The full selection allows a total background rejection for both PPS timing resolutions, but a better timing resolution always benefits the number of selected signal events. For every toy experiment the data frame will be slightly different because of the applied smearing within the pre-selection 4.2 procedure. This results in different sizes of input signal and background for the signal selection and thus different acceptance rates for each toy experiment. In average the calculated figure of merit (defined in equation 5) to select a correct signal event over the background estimate with the full selection is given in the last column of table 1:

Including station 1-4

PPS time resolution	Only kinematics	Kinematics & vertex position	**Full selection**
50 ps	≈ 1.19	≈ 1.11	$\mathbf{1.058 \pm 0.029}$
20 ps	≈ 1.19	≈ 1.03	$\mathbf{1.022 \pm 0.016}$

Table 1: Summary of results from the combination of the different signal selection criteria; only the "Full selection" is averaged over a larger number of toy experiments, the other figures of merit are exemplary for one single toy experiment.

This confirms that a better timing resolution corresponds to a narrower correlation and thus better signal to background separation. Compared to the result from the previous study [1] that accepted 17 events in total (12 Signal and 5 Background), the additional time measurement from the MTD improves the CEP signal to background separation a lot. For the current implementation with the three PPS stations the average significance to select a correct signal event over the background estimate is: 1.0. But for this scenario, with simulated MC data that includes roughly 1-2 days of HL-LHC running, there will be only between 2 (PPS resolution 50ps) and 4 (PPS resolution 20ps) accepted signal events due to the low PPS ξ acceptance. The three tracking station scenario allows in principle a full background exclusion but the statistics is, at least with this set of MC simulated data, too low to study the CEP and further any Beyond the Standard Model, Dark Matter or Higgs physics.

Based on the results of this project, the hypothetical station 4 scenario should be taken into account for the future HL-LHC operation. The future CMS PPS offers, with the additional timing measurement from the MTD, a unique possibility to study CEPs at the HL-LHC with the modest PPS timing resolution of 50ps, presumed the fourth PPS tracking station will be installed.

6 Acknowledgements

First I would like to thank the CERN Summer Students team for the organization of the digital program and the great opportunity to be part of it. I am very grateful for the awesome project that I was working on and even more for the outstanding supervision and guidance from Jonathon Hollar, Michael Pitt and Martijn Mulders. Jonathan and Michael been answering all my questions, helped me a lot with writing the selection code and they have been frequently available to discuss my doubts. I am also thanking my former roommate for the regular muffin and cake delivery to my door.

As grateful as I am for the human support, I have to include the good old gods:

Thank you, Fortunae !

References

[1] A. M. Sirunyan et al. "Observation of proton-tagged, central (semi)exclusive production of high-mass lepton pairs in pp collisions at 13 TeV with the CMS-TOTEM precision proton spectrometer". In: *Journal of High Energy Physics* 2018.7 (July 2018). ISSN: 1029-8479. DOI: `10.1007/jhep07(2018)153`. URL: `http://dx.doi.org/10.1007/JHEP07(2018)153`.

[2] CMS Collaboration. *The CMS Precision Proton Spectrometer at the HL-LHC – Expression of Interest*. 2021. arXiv: `2103.02752 [physics.ins-det]`.

[3] *Technical proposal for a MIP timing detector in the CMS experiment Phase 2 upgrade*. Tech. rep. Geneva: CERN, Dec. 2017. URL: `https://cds.cern.ch/record/2296612`.

[4] David Barney. "CMS Detector Slice". CMS Collection. Jan. 2016. URL: `https://cds.cern.ch/record/2120661`.

[5] Florian Bechtel and Peter Schleper. "The Underlying Event in Proton-Proton Collisions". In: (Aug. 2021).